

Radio Confusion on Cluster Sunyaev-Zel'dovich Effect

Huichun Lin¹, Tzihong Chiueh²

Department of Physics, National Taiwan University, Taipei 106, Taiwan

and

Xiang-Ping Wu³

National Astronomical Observatories, Chinese Academy of Sciences, Beijing 100012, China

ABSTRACT

We examine the expected radio confusion on the thermal Sunyaev-Zel'dovich (SZ) effect of galaxy clusters at 28.5 GHz and 90 GHz based on the cluster radio luminosity function (CRLF) at 1.4 GHz. With the observationally determined spectral index (α , where $S_\nu \propto \nu^{-\alpha}$) distribution, instead of a single average index $\langle\alpha\rangle$, we convert the cluster radio luminosity function at 1.4 GHz to the high frequency ones and estimate the total radio flux in a cluster. At 28.5 GHz, radio confusion is up to 10 ~ 100% for small clusters ($M \sim 2 \times 10^{14} M_\odot$) below redshift $z=1$, with more severe confusion for smaller and lower redshift clusters. By contrast, at 90 GHz the confusion is less than 10% for small clusters even at low redshifts.

Subject headings: cosmology: theory — galaxies: clusters: general — radio continuum: general

1. Introduction

The cosmic microwave background radiation (CMBR) provides a light source for exploration of the structure formation history. Before the CMBR photons reach the present

¹Email: deutsch@stella.astro.ncu.edu.tw

²Adjunct Research Fellow, Institute of Astronomy and Astrophysics, Academia Sinica, Taipei 106, Taiwan
Email: chiuehth@phys.ntu.edu.tw

³Email: wxp@bao.ac.cn

epoch, they interact with the hot diffuse ionized gas residing in the galaxy clusters over a wide range of redshifts. This process results in subtle changes to the CMBR spectrum due to the inverse Compton scattering, the so-called Sunyaev-Zel'dovich (SZ) effect (Sunyaev & Zel'dovich, 1972; see Birkinshaw 1999 and Carlstrom et al. 2000 for reviews). In the past two decades the detection of SZ effects has been reported at an increasing rate (Grego et al. 2000; Carlstrom et al. 2000; Joy et al. 2001; Grego et al. 2001) and this effect can therefore provide a realistic powerful probe for cosmological and cluster studies. Since the SZ flux is not affected by the distance but depends only on the intrinsic thermal energy of hot gases contained in the system, the SZ observation, in conjunction with observations of other wavelengths, such as X-ray emitted from intracluster gas, and optical weak lensing measurements, enables us to determine the cosmological parameters by studying the high redshift galaxy clusters. The SZ blank sky surveys have been suggested (Bartlett & Silk 1994; Barbosa et al. 1996). Several works follow (Bartlett 2000; Holder et al. 2000; da Silva et al. 2000; Kneissl et al. 2001; Fan & Chiueh 2001; Xue & Wu 2001), and have predicted how the SZ cluster counts can be related to cosmological parameters. In addition, several next generation interferometric arrays are either under construction or have been proposed, e.g., AMI (Kneissl et al. 2001), SZA (Carlstrom et al. 2001), and AMiBA (Lo et al. 2001).

Radio point sources or radio galaxies are usually found in the galaxy clusters. Therefore, the accuracy of the millimeter to centimeter wavelength observations of the SZ effect can be contaminated by the emission from radio sources (Loeb & Refregier 1997). Below 218 GHz, at which the thermal SZ effect becomes null, one measures the SZ intensity or flux decrement. The radio sources, however, produce excess emission so that one can underestimate the measured SZ decrement, yielding systematic errors in the estimate of cosmological parameters. This confusion has been estimated by Cooray et al. (1998, hereafter CGHJC), who observed toward Abell 2218 at 28.5 GHz and concluded that the correction to the Hubble constant is less than 6%. In addition to point sources, diffuse cluster radio sources, i.e. halos and relics, (e.g., Giovannini et al. 1993; Röttgering et al. 1997) also lead to confusion on the cluster SZ.

With the requirement of accurate SZ maps, the radio source subtraction becomes essential for the low brightness (order of 100 μ Jy and mJy) SZ measurements. For this reason, recent SZ observations are performed in combination with the measurements of radio sources (CGHJC; Komatsu et al. 1999; Pointecouteau et al. 2001). While one may remove strong sources as they can be detected above the flux limit, the faint sources below the flux threshold blend with the SZ signal, and result in inaccuracy. However, there have not been systematic surveys on the radio sources in high redshift clusters nor systematic surveys at frequencies higher than 30 GHz. In fact, the high-frequency (e.g. 90 GHz) radio survey at the mJy flux limit is a formidable task, as the present telescopes are not sufficiently efficient

in conducting an unbiased survey with a wide field coverage and high sensitivity. In view of the lack of reliable information for estimating the radio contamination on the SZ cluster surveys at high frequencies, such as AMiBA (90 GHz), we are motivated to derive an empirical high-frequency cluster radio luminosity function (CRLF) by synthesizing available low-frequency data (Ledlow & Owen 1996, hereafter LO96; Slee et al. 1996, hereafter SRA96, and CGHJC). Unfortunately, the spectral evolution of radio sources is rather uncertain. Due to the uncertainties of redshift evolution, it is reasonable, as a first attempt, to adopt a no-evolution hypothesis to evaluate the radio flux in high redshift clusters. In this paper we aim to calculate the expected confusion of high-frequency radio point sources on the cluster SZ effect over substantial redshift and cluster mass ranges. In section 2, we briefly review the formulation of the SZ flux. Section 3 predicts the high frequency cluster radio luminosity functions (CRLFs) based on low frequency surveys. The expected high frequency radio flux are calculated in section 4. Finally, the conclusion is given in section 5. Throughout this paper, we use $H_0 = 65 \text{ km s}^{-1} \text{ Mpc}^{-1}$, $\Omega_M = 0.35$, and $\Omega_\Lambda = 0.65$.

2. SZ Flux

One may evaluate the total SZ flux by the procedure as follows (see also Barbosa et al. 1996, Xue & Wu 2001). For the CMB radiation passing through the intracluster hot gas, the change in CMB intensity by thermal SZ effect is

$$\Delta I_\nu = j_\nu(x) \int \left(\frac{kT_e}{m_e c^2} \right) \sigma_T n_e dl, \quad (1)$$

where m_e is the electron rest mass, n_e is the electron number density, T_e is the electron temperature, and σ_T is the Thomson cross section. $j_\nu(x)$ represents the spectral dependence

$$j_\nu(x) = 2 \frac{(kT_0)^3}{(h_p c)^2} \frac{x^4 e^x}{(e^x - 1)^2} \left[x \coth \left(\frac{x}{2} \right) - 4 \right], \quad (2)$$

in which $x \equiv h_p \nu / kT_0$ and $T_0 = 2.728 \text{ K}$ is the CMB temperature. For $\nu = 90 \text{ GHz}$, $x \approx 1.58$. The total SZ flux of a cluster at redshift z is the integral of the intensity over the solid angle subtended by the cluster

$$S_\nu = \frac{j_\nu(x)}{D_A^2(z)} \left(\frac{\sigma_T}{m_e c^2} \right) \int kT_e n_e dV, \quad (3)$$

where D_A is the angular diameter distance to the cluster. If we assume the gas is isothermal, then the total SZ flux depends only on the electron number, which can be replaced by the

gas mass of the cluster. Introduce the gas fraction $f_b = M_{\text{gas}}/M_{\text{vir}}$, where M_{vir} is the virial mass of the cluster, then the equation above becomes

$$S_\nu = \frac{j_\nu(x)}{D_A^2(z)} \left(\frac{kT_e}{m_e c^2} \right) \left(\frac{f_b \sigma_T}{\mu_e m_p} \right) M_{\text{vir}}, \quad (4)$$

where $\mu_e = 2/(1 + X)$, and $X=0.768$ is the hydrogen mass fraction in the primordial abundances of hydrogen and helium.

Define R_{vir} as the radius of the cluster within which the mean density is Δ_c times the critical density of the universe ρ_c at a certain redshift, i.e., $M_{\text{vir}} = 4\pi R_{\text{vir}}^3 \rho_c \Delta_c / 3$, then the relation between temperature and mass is (Bryan & Norman 1998)

$$kT_e = 1.39 f_T \left(\frac{M_{\text{vir}}}{10^{15} M_\odot} \right)^{2/3} [h^2 \Delta_c E(z)^2]^{1/3} \text{ keV}, \quad (5)$$

where $E(z)^2 = \Omega_M(1+z)^3 + \Omega_K(1+z)^2 + \Omega_\Lambda$, $\Omega_K = 1 - \Omega_M - \Omega_\Lambda$, and the redshift-dependent Hubble constant $H(z) = 100hE(z) \text{ km s}^{-1} \text{ Mpc}^{-1}$. f_T is a normalization factor obtained by numerical simulations and about 1. Δ_c is the density contrast of the virialized spherical halo to the critical density of the universe at that redshift, which can be fitted as (Eke et al. 1996) $\Delta_c = 18\pi^2 + 82[\Omega(z) - 1] - 39[\Omega(z) - 1]^2$ for $\Omega_K = 0$, where $\Omega(z) = \Omega_M(1+z)^3/E^2(z)$.

The gas fraction f_b varies with the cluster temperature by the empirical formula (Mohr et al. 1999)

$$f_{b,50} = (0.207 \pm 0.011) \left(\frac{kT}{6 \text{ keV}} \right)^{0.34 \pm 0.22}, \quad (6)$$

where the subscript 50 denotes $h=0.5$. We may scale f_b by $f_b = f_{b,50} h_{50}^{-1.5}$ (White et al. 1993), and Eq.(4) and (6) will be used to compare with the radio flux calculated in the next section, so as to determine the radio confusion on the SZ flux. The reason for incorporating the temperature dependence of f_b is as follows. It is likely that preheating by supernovae and/or AGNs provides nongravitational heating to the intracluster gas, which makes the distribution of the hot gas extend to large radii (Wu et al. 1998, 2000). The effect is more significant in poor clusters than in rich ones because the former have a shallow gravitational potential, as evidenced by the steepening of the L_x - T relation (David et al. 1993; Wu et al. 1999) as well as the excess entropy in galaxy clusters (Ponman et al 1999).

3. CRLF and Radio Flux

To estimate the total flux of the radio galaxies in clusters, we adopt the CRLF given by LO96 (Paper VI). They did a series of surveys on a large sample of radio galaxies in Abell

clusters using VLA, e.g., in Paper IV (Ledlow & Owen 1995a, hereafter LO95a), where the radio sample and cluster properties were presented; in Paper V (Ledlow & Owen 1995b), they did optical observation and investigated the optical properties toward their radio sample.

In LO96, the CRLF is for a complete sample of Abell clusters with $z < 0.09$ and can be fitted by a continuous broken power law

$$\log f_{1.4} \equiv \log \frac{N_{\text{radio}}(\log P_{1.4})}{N_{\text{opt}}} = a + b \log P_{1.4}, \quad (7)$$

in which N_{opt} represents the number of galaxies over all magnitudes brighter than -20.5 within 0.3 Abell radius of the cluster center and $N_{\text{radio}}(\log P_{1.4})$ represents the number of radio galaxies which emit the radio power $P_{1.4}$ at 1.4 GHz. The coefficients b and a are fitted with the central values as -0.15 and 1.77 for $P_{1.4} < 10^{24.8} \text{ WHz}^{-1}$, and -1.43 and 33.67 for $P_{1.4} > 10^{24.8} \text{ WHz}^{-1}$, respectively.

We evaluate the predicted cluster radio luminosity functions at other frequencies, f_ν , based on the 1.4 GHz survey by convoluting $f_{1.4}$ with the spectral index distribution $n(\alpha)$ as

$$\log f_\nu = \int \int (\log f_{1.4}) n(\alpha) \delta \left[\log P_{1.4} - \log P_\nu - \alpha \log \left(\frac{\nu}{1.4 \text{ GHz}} \right) \right] d\alpha d \log P_{1.4}, \quad (8)$$

where $f_{1.4}$ is the luminosity function given by Eq.(7). The spectral index distributions $n(\alpha)$ that we adopt are fitted by two Gaussians and normalized as

$$n(\alpha) = \begin{cases} 0.21e^{-0.72(\alpha-1.14)^2} + 1.06e^{-11.0(\alpha-0.98)^2}; & \text{SRA96 sample} \\ 0.95e^{-8.33(\alpha-1.02)^2} + 0.44e^{-3.41(\alpha-0.57)^2}; & \text{CGHJC sample} \end{cases}, \quad (9)$$

and are shown in Figure 1. The circles are from SRA96 and the crosses are from CGHJC. The two distributions are normalized to their total number of sources for comparison. The SRA96 sample contains 254 radio sources and its $n(\alpha)$ appears more regular than that of CGHJC sample, which contains 53 sources (α available) only in very massive clusters ($M > 10^{15} M_\odot$). Moreover, the spectral index in SRA96 sample is determined at lower frequencies ($1.5 \text{ GHz} < \nu < 4.9 \text{ GHz}$), whereas CGHJC sample at higher frequencies ($1.4 \text{ GHz} < \nu < 28.5 \text{ GHz}$). Despite these differences, the two $n(\alpha)$ do not differ much, at least in the main body of the distribution. We show in Figure 2 the predicted CRLFs using SRA96's $n(\alpha)$ at $\nu = 28.5(1+z) \text{ GHz}$, and $90(1+z) \text{ GHz}$ for $z=0.25$, respectively. Note that the cosmological expansion has been considered, where the frequency of the predicted function has a redshift dependence $\nu = \nu_0(1+z)$, where ν_0 is observed frequency. For simplicity in calculating the total flux, we fit the luminosity-weighted CRLFs by a broken power law,

$$\log (P_\nu f_\nu) = \begin{cases} C_1(\nu) + \gamma_1(\nu) \log P_\nu; & \log P < \log P_b \\ C_2(\nu) + \gamma_2(\nu) \log P_\nu; & \log P > \log P_b \end{cases}, \quad (10)$$

where $\log P_b$ is the break point of a continuous luminosity-weighted CRLF, and the fit coefficients are list in the Table 1. We see that both the break points of SRA96 and CGHJC vary slightly with frequency, and that the peak power of radio sources decreases with increasing frequency. But the fit coefficients from the two groups are not in good agreement, as shown below. This is due to that the sample of CGHJC has flatter spectra, and the resulting power is higher.

Assuming neither evolution effect on the spectral indices nor on the intrinsic brightness of radio sources, we obtain the best fit for the frequency dependence of these CRLFs coefficients,

$$\begin{cases} C_1(\nu) = 1.68 + 0.015\nu - 2.1 \times 10^{-5}\nu^2 \\ \gamma_1(\nu) = 0.85 - 0.0010\nu + 1.91 \times 10^{-6}\nu^2 \\ C_2(\nu) = 23.84 + 9.92e^{-0.015\nu} \\ \gamma_2(\nu) = -0.44e^{-0.007\nu} - 2.9 \times 10^{-4}\nu \end{cases} ; \text{ SRA96's } n(\alpha), \quad (11)$$

and

$$\begin{cases} C_1(\nu) = 2.68 - 0.95e^{-0.015\nu} \\ \gamma_1(\nu) = 0.85e^{-0.0027\nu} + 1.49 \times 10^{-3}\nu \\ C_2(\nu) = 30.42 + 3.29e^{-0.025\nu} \\ \gamma_2(\nu) = -0.43e^{-0.0022\nu} - 6.14 \times 10^{-4}\nu \end{cases} ; \text{ CGHJC's } n(\alpha). \quad (12)$$

Figure 3 shows how the coefficients depend on frequencies and their best-fit curves. One may construct the CRLF of any redshift by interpolating the emitted frequency ν , as $\nu_0(1+z)$, where ν_0 is the observed frequency.

Taking an integral over the radio power range from 10^{17} to 10^{26} WHz^{-1} and multiplying it by the total number of cluster galaxies, we have the total radio power emitted from the radio galaxies within a single cluster

$$P_\nu^{\text{tot}} = N_{\text{vir}} \int P_\nu f_\nu dP_\nu, \quad (13)$$

where N_{vir} is the number of galaxies in a cluster of mass M_{vir} . We estimate the total number of radio sources in a cluster by the mass-to-number relation for a given cluster mass M_{vir} (Carlberg et al. 1996). They use the CNOC Cluster Survey to derive the $M_{\text{vir}}/N_{\text{gal}}$ ratios using the sample with r-band absolute-magnitude limits from $M_r^K = -18.0$ to -20.0 . To be consistent with N_{opt} in Eq.(7), which has the optical limiting magnitude at -20.5 , we fit the mass-to-number relation derived by Carlberg et al. (1996), and extrapolate the limiting magnitude to $M_r^K = -20.5$ to obtain $M_{\text{vir}}/N_{\text{gal}} \simeq 1.5 \times 10^{13} h^{-1} M_\odot$. For a given cluster mass M_{vir} , we take this N_{gal} as the number of galaxies N_{vir} in Eq.(13).

To be compared with SZ flux, the total radio flux observed at frequency ν_0 at redshift z can be evaluated from the total power at frequency ν as

$$S_{\nu_0, \text{obs}} = \frac{P_{\nu}^{\text{tot}}(1+z)}{4\pi D_L^2(z)}, \quad (14)$$

where $D_L(z)$ is the luminosity distance to redshift z , $D_L(z) = (1+z)^2 D_A(z)$, and radio sources are assumed to have no evolution. We combine Eq.(4) and Eq.(14) to determine the confusion.

4. Result

In Figure 4, we plot the total radio flux v.s. the virial mass of a galaxy cluster (or group) at redshift $z=0.25, 0.5$, and 1.0 . The left panels are for the observed frequency 28.5 GHz (operated in SZA) and the right for 90 GHz (operated in AMiBA). The 1σ error bars result primarily from the variance of the predicted luminosity-weighted function $P_{\nu}f_{\nu}$, and are much larger than the observational errors of $f_{1.4}$ and $n(\alpha)$, which are neglected. These large error bars are due to the broad scattering of the distribution of the spectral index α . As a consistency check, we compared our estimate flux at 28.5 GHz with the CGHJC sources in Figure 4, and at 1.4 GHz with the LO95a sources in Figure 5. The dash lines are our predicted mean flux, and the data points are the radio flux provided by LO95a. We have investigated the redshift and the X-ray temperature of their selected clusters (c.f. Ebeling et al. 1996, 1998) and converted the cluster temperature to the virial mass by Eq.(5) to obtain the coordinates of the data points in Figure 4 and 5. It shows that the total radio flux at 28.5 GHz of most but few clusters in their sample are consistent with our predictions within 1σ . The same agreement is also found at 1.4 GHz. Since the measured clusters of CGHJC are massive, their sample may have some selection bias. It may result in asymmetry in their spectral index distribution $n(\alpha)$, leading to the predicted radio flux higher than those from SRA96, by almost a constant factor $\sim 2.5 - 3$ throughout all frequencies of interest. It is instructive to examine the averaged spectral index $\langle\alpha\rangle$ derived from each individual $n(\alpha)$ given by SRA96 and by CGHJC. It is found that

$$\langle\alpha\rangle \equiv \frac{\ln[\int (P_{\nu}f_{\nu})d\log P_{\nu} - \text{const.}]}{\ln \nu} = \begin{cases} -1.15; & \text{for SRA96} \\ -0.9; & \text{for CGHJC} \end{cases} \quad (15)$$

The $\langle\alpha\rangle$ value for CGHJC is somewhat higher than that for SRA96, but is lower than the $\langle\alpha\rangle$ value, -0.77 , given by CGHJC based solely on their 53 sources. The flatter spectrum signifies the somewhat different radio sources in massive clusters from in average clusters.

The flux ratios v.s. the cluster mass are shown in Figure 6. Note that the SZ flux are represented in *positive* values. The flux ratio decreases with mass, since the SZ flux increases with M_{vir} faster than the radio flux does. The flux ratio also decreases with redshift under the presently adopted no-evolution hypothesis. Moreover, at $\nu \sim 30$ GHz, the radio flux are higher and the SZ flux are lower than those at 90 GHz, and therefore the flux ratios of the two frequencies differ by a large margin. In SZ surveys for cluster mass ranging from $M \sim 2 \times 10^{14} M_{\odot}$ to $2 \times 10^{15} M_{\odot}$, the radio contamination at 30 GHz should be a serious concern for small clusters even at $z=1$ ($\sim 10\%$), whereas the contamination for small clusters at 90 GHz is lower than 10% even at $z=0.25$.

5. Conclusion

We study the CRLFs from 1.4 GHz to 180 GHz, based on the flux-limited 1.4 GHz observation in conjunction with studies of radio spectral index at higher frequencies. The lack of comprehensive radio spectra of galaxy clusters remains a problem for predicting the radio confusion on the cluster SZ effect. In our analysis, the cluster radio luminosity functions at high frequencies are obtained by converting the observed low-frequency ones with the observed spectral index distributions of radio sources. We obtain the frequency dependence of the CRLF from two spectral index studies. Assuming that CRLFs do not evolve, the redshift dependence of CRLFs can be derived as well. Based on this information, we calculate the total flux of radio point sources in a cluster for mass ranging from $M = 1 \times 10^{14} M_{\odot}$ to $5 \times 10^{15} M_{\odot}$ at high frequencies and various redshifts. Apart from few exceptional clusters, our predictions agree with LO95a (at 1.4 GHz) and CGHJC (at 28.5 GHz) observations in a self-consistent manner.

We also give estimates of the confusion from radio point sources to the SZ flux. As demonstrated in Figure 6, the radio confusion to lower frequency ($\nu \approx 30$ GHz) SZ measurements poses a severe problem for cluster of $M \lesssim 10^{15} M_{\odot}$, whereas at higher frequency ($\nu \approx 90$ GHz) the radio confusion causes less a problem even for small clusters ($M \sim 10^{14} M_{\odot}$). For observed frequencies substantially lower than 30 GHz, such as 15 GHz proposed to be operated at AMI, one may use Eq.(15) to estimate the expected level of radio confusion. Take $\langle \alpha \rangle = -1$; the 15 GHz radio flux is twice higher but the SZ flux is 4 times weaker (due to the ν^2 Rayleigh-Jeans tail) than those in the 30 GHz observation, and the confusion flux ratio becomes 8 times higher than that of 30 GHz.

The estimate for the expected total confusion to a cluster of given virial mass can be translated to the expected loss of SZ signals, which results in reducing the cluster count and in turn affecting the inferred values of cosmological parameters. As has already been

demonstrated, the amplitude of density fluctuations averaged over $8h^{-1}$ Mpc, σ_8 , is most sensitive to the SZ cluster count (Fan & Chiueh 2001). The radio confusion thus yields a lower value of the inferred σ_8 . Nevertheless, with the aid of a sensitive telescope for pointed observation, the radio confusion can partially be removed by subtraction, when the radio sources are sufficiently strong. However weak radio sources remain to be a problem as they are bound to blend into the SZ signals and cannot be subtracted away. The spectral-index distribution $n(\alpha)$ can in principle reveal the relative population of strong and weak sources at high frequencies. But this problem can be assessed in a different way. We have compared the observed radio flux of CGHJC (28.5 GHz) and LO95a (1.4 GHz) with the predicted total radio flux in Figure 4 and 5, and the data show large scatters around the expected flux. It suggests that many sources are weak and can be difficult to get removed by subtraction. Therefore, a good SZ observing strategy is probably to set the SZ flux limit substantially higher than the expected flux of radio sources in a cluster. For 90 GHz observations, a mJy flux limit is adequate for this purpose.

This work was supported in part by NSC 90-2112-M-002-026 from the National Science Council, R.O.C. and by the National Science Foundation of China.

REFERENCES

- Barbosa, D., Bartlett, J. G., Blanchard, A., & Oukbir, J. 1996, A&A, 314, 13
- Bartlett, J. G. 2000, A&A, in press
- Bartlett, J. G., & Silk, J. 1994, ApJ, 423, 12
- Birkinshaw, M. 1999, Phys. Rep., 310, 97
- Bryan, G. L., & Norman, M. L. 1998, ApJ, 495, 80
- Carlberg, R. G., Yee, H. K. C., Ellingson, E., Abraham, R., Gravel, P., Morris, S., & Pritchet, C. J. 1996, ApJ, 462, 32
- Carlstrom, J. E., Joy, M., Grego, L., Holder, G., Holzapfel, W. L., LaRoque, S., Mohr, J. J., & Reese, E. D. 2000, in IAP July 2000, *Constructing the Universe with Clusters of Galaxies*, eds. F. Durret, & G. Gerbal, in prep, astro-ph/0103480
- Carlstrom J. E. et al., 2001, <http://astro.uchicago.edu/SZE> (SZA)
- Cooray, A. R., Grego, L., Holzapfel, W. L., Joy, M., & Carlstrom, J. E. 1998, AJ, 115, 1388
- da Silva, A. C., Barbosa, D., Liddle, A. R., & Thomas, P.A. 2000, MNRAS, 317, 37
- David, L. P., Slyz, A., Jones, C., Forman, W., Vrtillek, S. D., & Arnaud, K. A. 1993, ApJ, 412, 479
- Ebeling, H., Voges, W., Böhringer, H., Edge, A. C., Huchra, J. P., & Briel, U. G. 1996, MNRAS, 281, 799
- Ebeling, H., Edge, A. C., Böhringer, H., Allen, S. W., Crawford, C. S., Fabian, A. C., Voges, W., & Huchra, J. P. 1998, MNRAS, 301, 881
- Eke, V. R., Cole, S., & Frenk, C. S. 1996, MNRAS, 282, 263
- Fan, Z., & Chiueh, T. 2001, ApJ, 550, 547
- Giovannini, G., Feretti, L., Venturi, T., Kim, K.-T., & Kronberg, P. P. 1993, ApJ, 406, 339
- Grego, L., Carlstrom, J. E., Joy, M. K., Reese, E. D., Holder, G. P., Patel, S., Cooray, A. R., & Holzapfel, W. L. 2000, ApJ, 539, 39
- Grego, L., Carlstrom, J. E., Reese, E. D., Holder, G. P., Holzapfel, W. L., Joy, M. K., Mohr, J. J., & Patel, S. 2001, ApJ, 552, 2

- Holder, G. P., Mohr, J. J., Carlstrom, J. E., Evrard, A. E., & Leitch, E. M. 2000, ApJ, 544, 629
- Joy, M., LaRoque, S., Grego, L., Carlstrom, J. E., Dawson, K., Ebeling, H., Holzapfel, W. L., Nagai, D., & Reese, E. D. 2001, ApJ, 551, L1
- Kneissl, R., Jones, M. E., Saunders, R., Eke, V. R., Lasenby, A. N., Grainge, K., and Cotter, G. 2001, MNRAS, 328, 783
- Komatsu, E., Kitayama, T., Suto, Y., Hattori, M., & Kawabe, R. 1999, ApJ, 516, L1
- Ledlow, M. J., & Owen, F. N. 1995a, AJ, 109, 3 (Paper IV)
- Ledlow, M. J., & Owen, F. N. 1995b, AJ, 110, 5 (Paper V)
- Ledlow, M. J., & Owen, F. N. 1996, AJ, 112, 9 (Paper VI)
- Lo, K. Y., Chiueh, T., Liang, H., Ma, C. P., Martin, R., Ng, K.-W., Pen, U. L., & Subramanyan, R. 2001. In IAU Symp. 201, *New Cosmological Data and the Values of the Fundamental Parameters*, eds. A. Lasenby, A. Wilkinson, & A. W. Jones, in prep, astro-ph/0012282
- Loeb, A., & Refregier, A. 1997, ApJ, 476, L59
- Mohr, J. J., Mathiesen, B., & Evrard, A. E. 1999, ApJ, 517, 627
- Pointecouteau, E., Giard, M., Benoit, A., Désert, F. X., Bernard, J. P., Coron, N., & Lamarre, J. M. 2001, ApJ, 552, 42
- Ponman, T. J., Cannon, D. B., & Navarro, J. F. 1999, Nature, 397, 135
- Röttgering, H., Wieringa, M., Hunstead, R., & Ekers, R. 1997, MNRAS, 290, 577
- Slee, O. B., Roy, A. L., & Andernach, H. 1996, Australian J. Phys., 49, 977
- Sunyaev, R. A., & Zel’dovich, Y. 1972, Comments Astrophys. Space Phys., 4, 173
- White, S. D. M., Navarro, J. F., Evrard, A. E., & Frenk, C. S. 1993, Nature, 366, 429
- Wu, K. K. S., Fabian, A. C., & Nulsen, P. E. J. 1998, MNRAS, 301, L20
- Wu, K. K. S., Fabian, A. C., & Nulsen, P. E. J. 2000, MNRAS, 318, 889
- Wu, X. P., Xue, Y. J., & Fang, L. Z. 1999, ApJ, 524, 22

Xue, Y. J., & Wu, X. P. 2001, ApJ, 552, 452

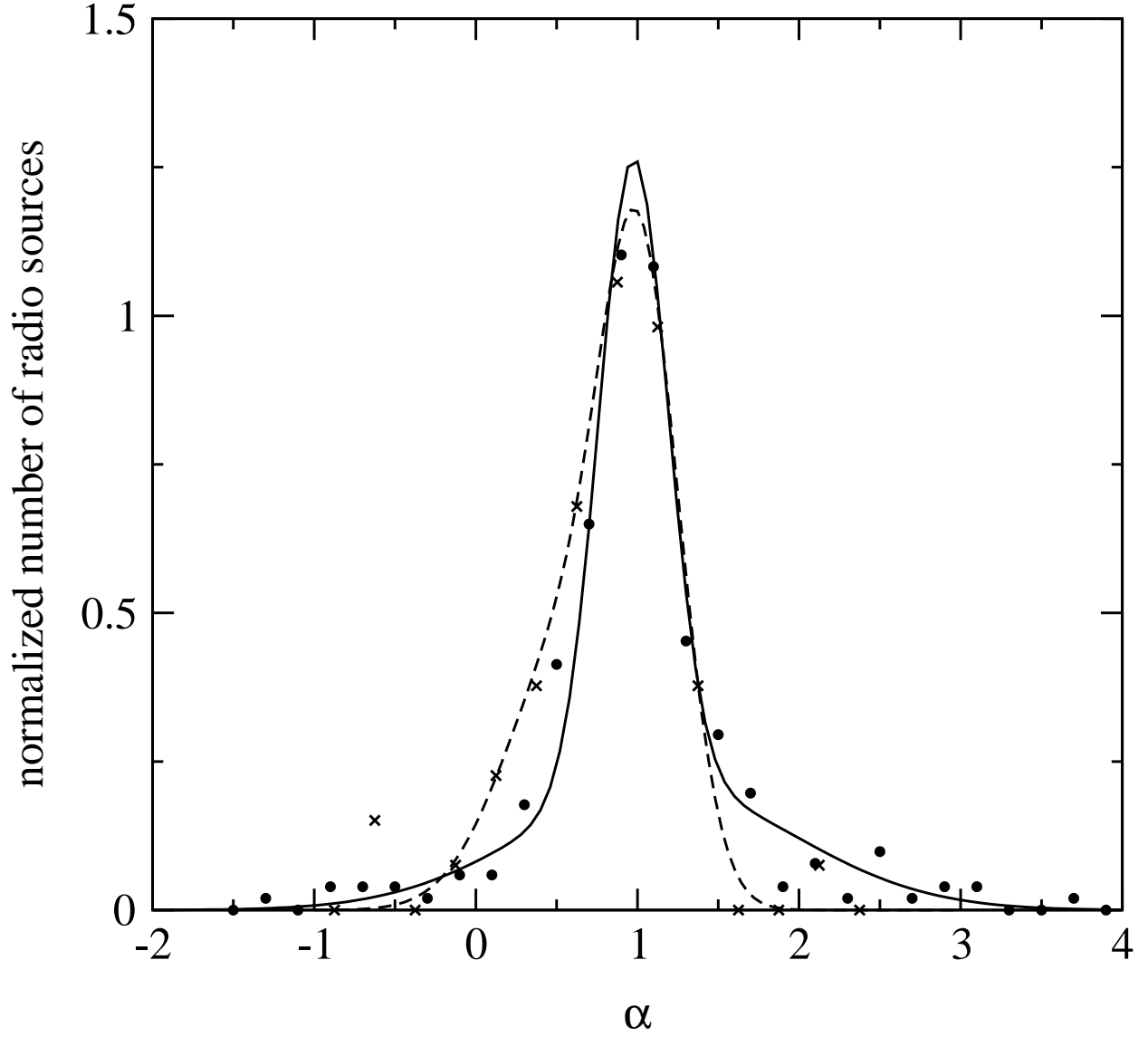


Fig. 1.— Normalized spectral index distribution of radio sources. The circles are from SRA96 (254 sources) and the solid line is the best fit; while the crosses are from CGHJC (53 sources) and the dash line is the best fit. CGHJC sample is biased toward very massive clusters ($> 10^{15} M_{\odot}$) and the spectral index distribution is more irregular at low and high α than that of SRA96.

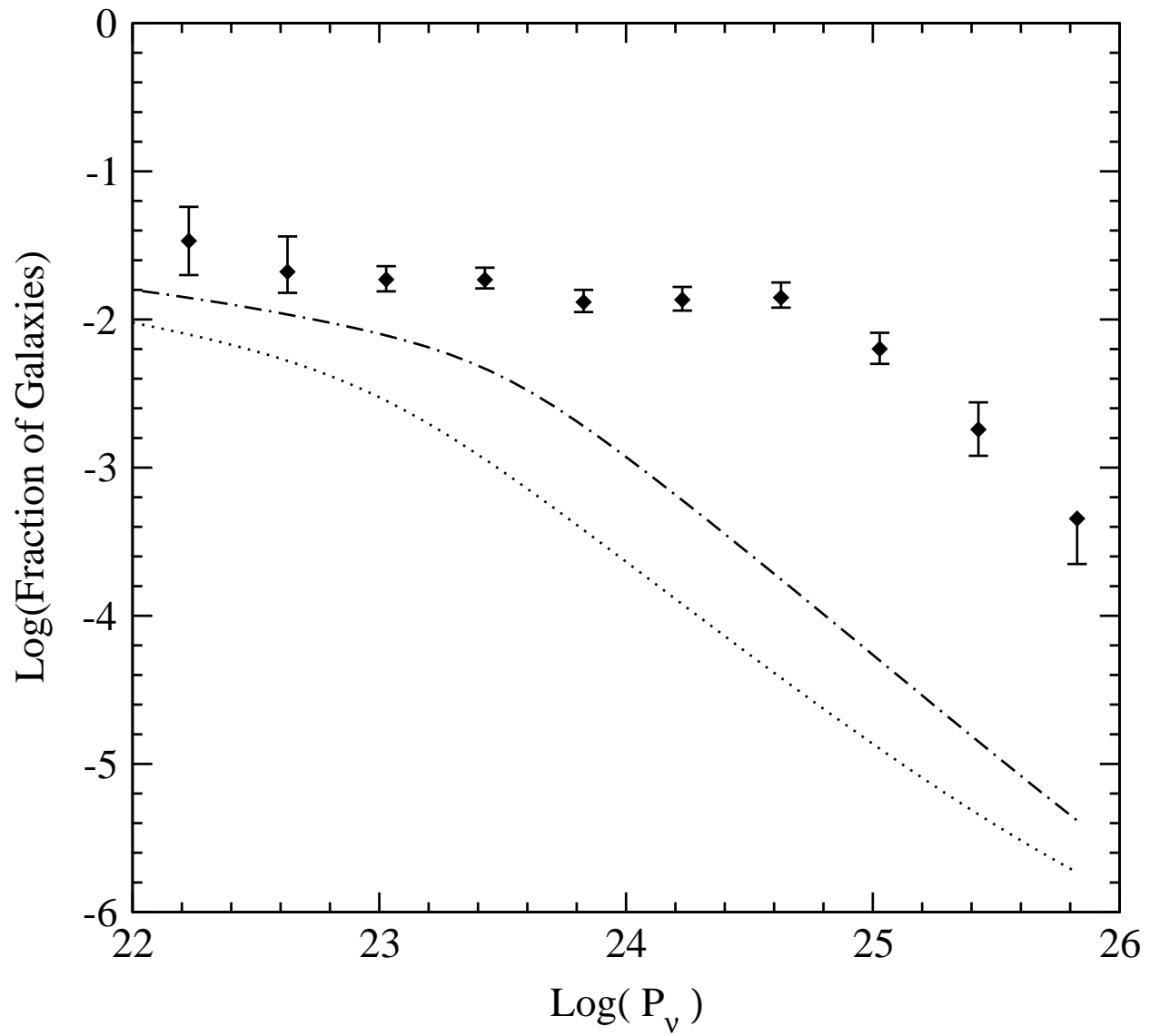


Fig. 2.— Predicted cluster radio luminosity functions at $\nu=28.5(1+z)$ GHz (the dash-dotted lines), and at $90(1+z)$ GHz (the dotted lines) for $z=0.25$. The data points are at 1.4 GHz from LO96.

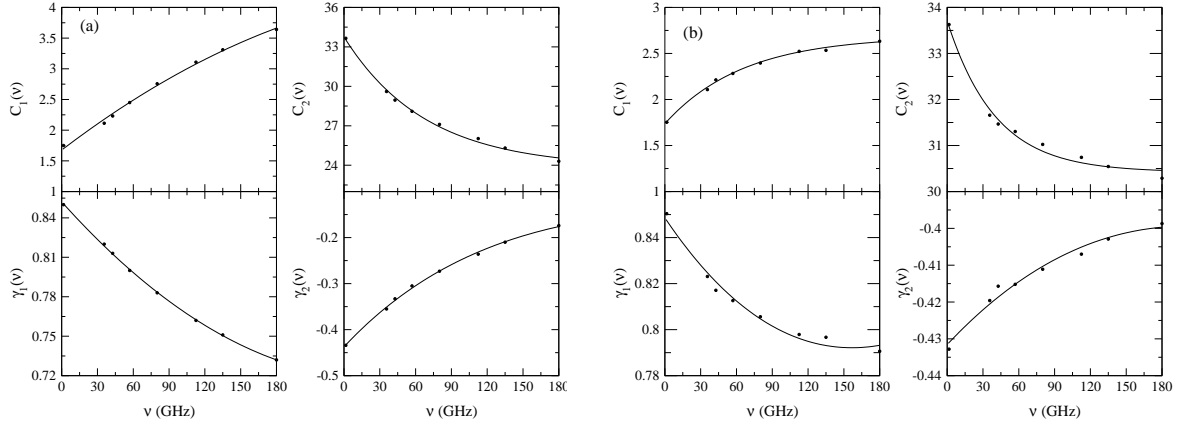


Fig. 3.— Coefficients of the luminosity-weighted CRLFs $[\log P_\nu f_\nu]$ from (a)SRA96's $n(\alpha)$, and (b)CGHJC's $n(\alpha)$ in frequency.

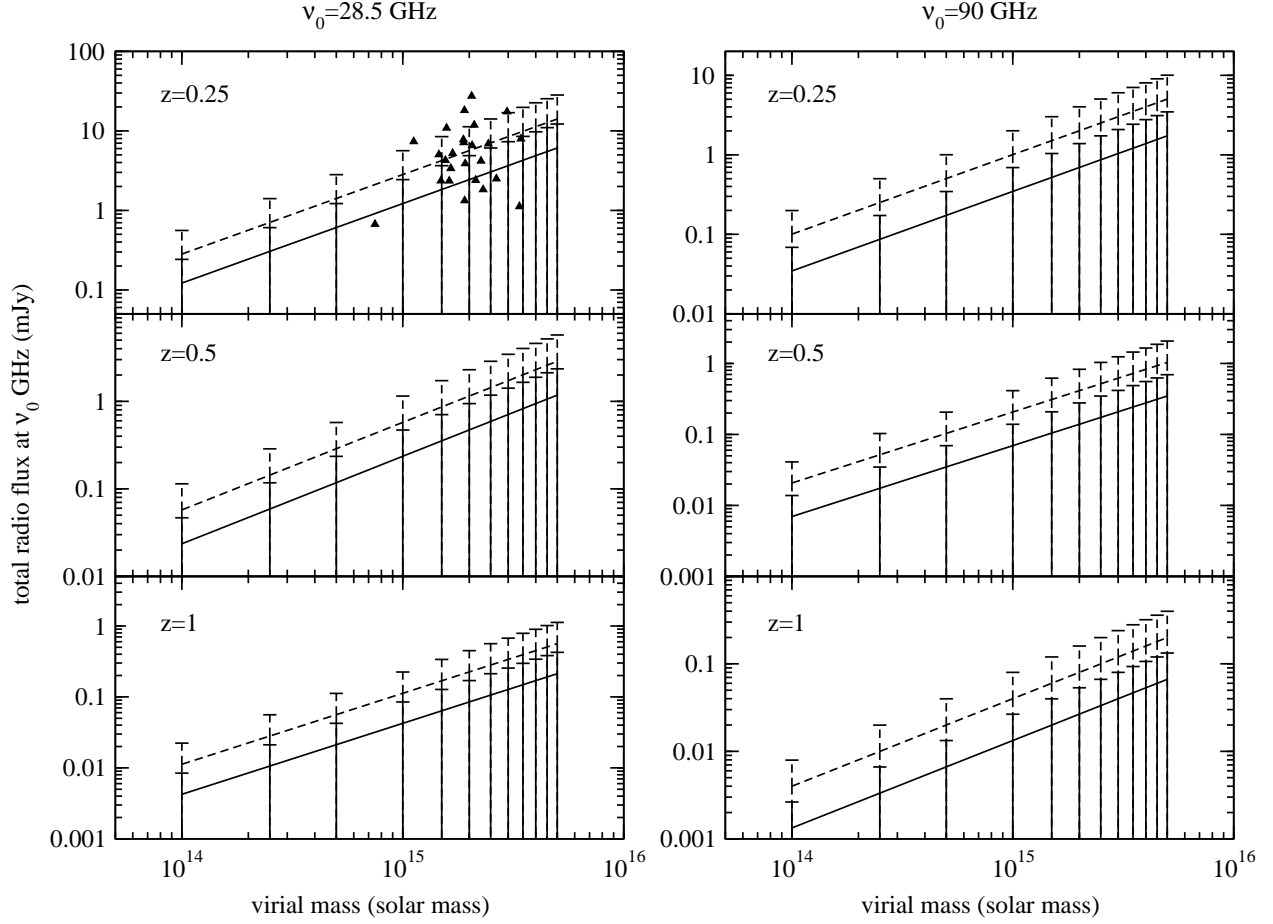


Fig. 4.— Total radio flux at $\nu = 28.5$ GHz, 90 GHz in cluster virial mass with redshifts $z = 0.25, 0.5, 1.0$, respectively. The solid lines are converted from SRA96's $n(\alpha)$, and the dash lines are from CGHJC. Triangles represent the radio flux of 25 clusters below $z = 0.3$ in CGHJC.

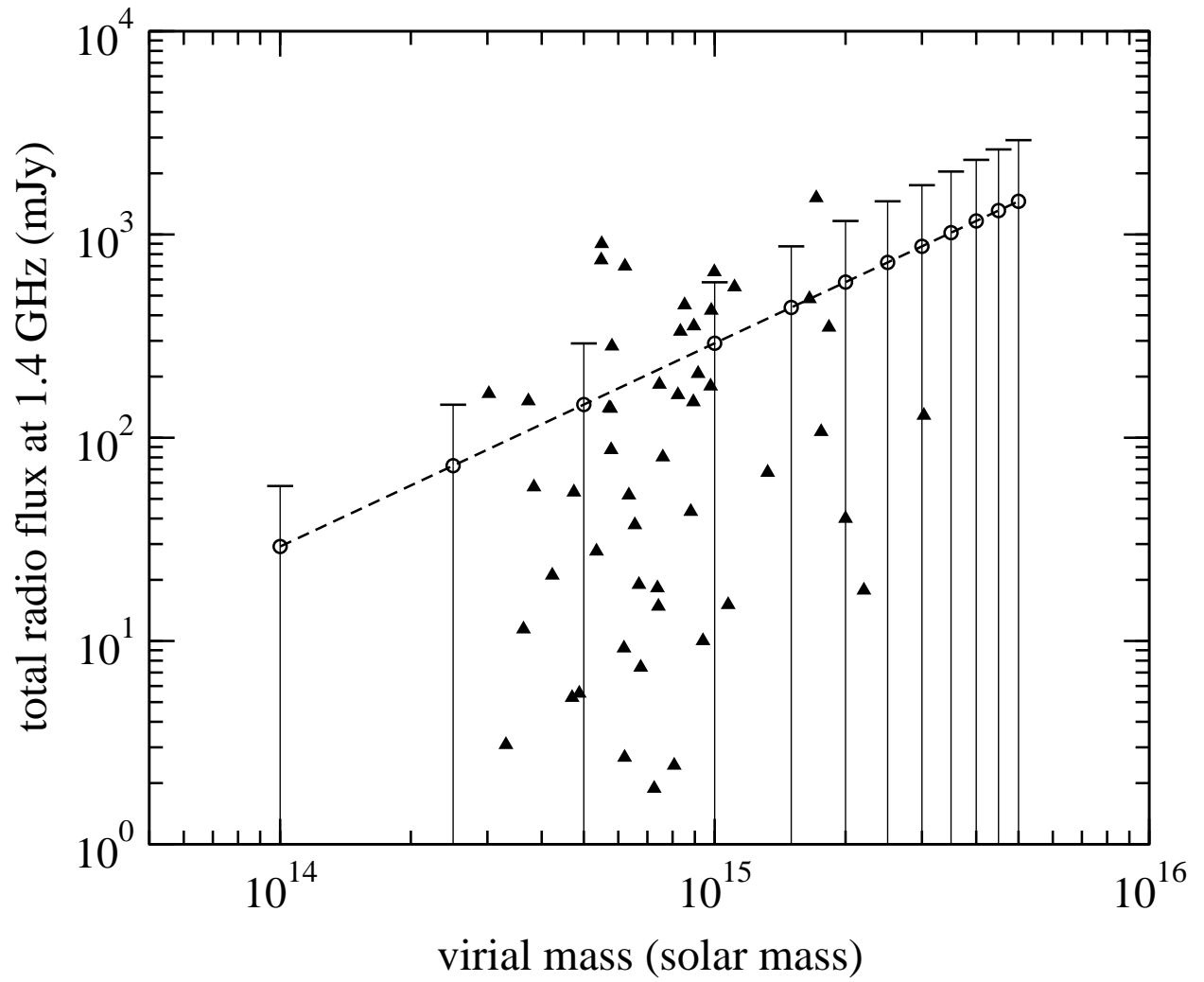


Fig. 5.— Total radio flux at 1.4 GHz from our predicted CRLFs. The data points are boosted up to $z=0.09$ from LO95a.

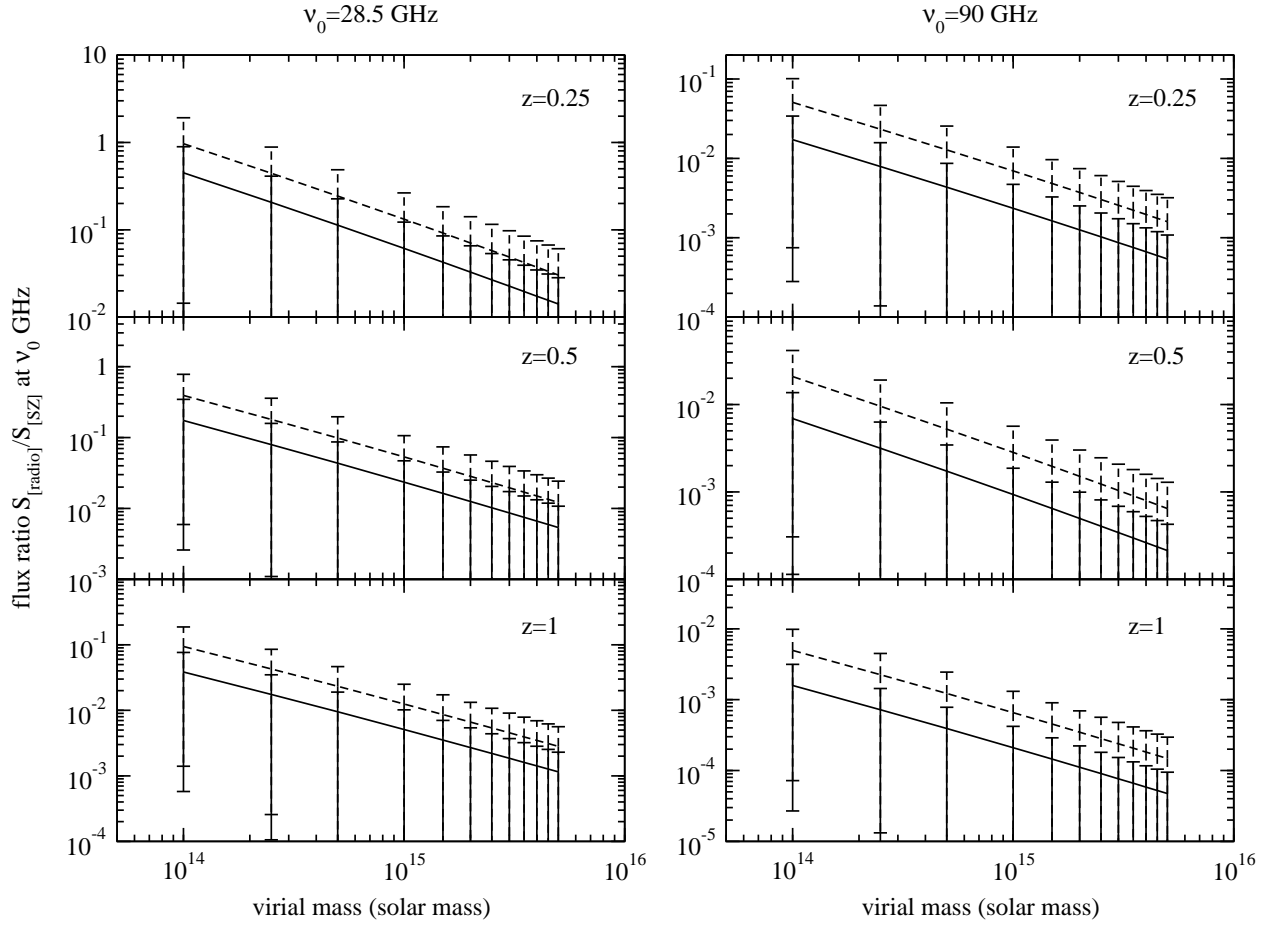


Fig. 6.— Flux ratios at $\nu=28.5$ GHz, 90 GHz in cluster virial mass with redshift $z=0.25$, 0.5, 1.0, respectively. The curves are the same as the former.

Table 1: Fit parameters for the dependence of the luminosity-weighted CRLFs $[\log P_\nu f_\nu]$ from $n(\alpha)$ in SRA96 and CGHJC, respectively.

Author	ν_0 GHz	z	ν GHz	C_1	γ_1	C_2	γ_2	$\log P_b$
SRA96	1.4	0.09	1.526	1.75	0.85	33.65	−0.43	24.8
	28.5	0.25	35.625	2.11	0.82	29.61	−0.36	23.4
	28.5	0.5	42.75	2.23	0.81	28.95	−0.33	23.3
	28.5	1.0	57.0	2.45	0.80	28.10	−0.31	23.2
	40.0	1.0	80.0	2.76	0.78	27.11	−0.27	23.1
	90.0	0.25	112.5	3.11	0.76	26.03	−0.24	23.0
	90.0	0.5	135.0	3.31	0.75	25.31	−0.21	22.9
	90.0	1.0	180.0	3.64	0.73	24.30	−0.17	22.8
CGHJC	1.4	0.09	1.526	1.75	0.85	33.63	−0.43	24.8
	28.5	0.25	35.625	2.11	0.82	31.66	−0.42	23.8
	28.5	0.5	42.75	2.21	0.82	31.47	−0.42	23.7
	28.5	1.0	57.0	2.28	0.81	31.30	−0.42	23.6
	40.0	1.0	80.0	2.40	0.81	31.02	−0.41	23.5
	90.0	0.25	112.5	2.52	0.80	30.74	−0.41	23.4
	90.0	0.5	135.0	2.53	0.80	30.55	−0.40	23.3
	90.0	1.0	180.0	2.63	0.79	30.29	−0.40	23.2